1526

Altered Large-Scale Brain Networks in Mesial Temporal Lobe Epilepsy Based on Dynamic Causal Modeling

Alireza Fallahi[1], Fatemeh Salimi[2], Fatemeh Eyvazi[3], Narges Hosseini Tabatabaei[4], Mohammad-Reza Ay[2], and Mohammad-Reza Nazem-Zadeh[2]

[1]Shahed University, Tehran, Iran (Islamic Republic of), [2]Tehran University of Medical Sciences, Tehran, Iran (Islamic Republic of), [3]Institute for cognitive science studies, Shahid Beheshti University, Tehran, Iran (Islamic Republic of), [4]Brain and Spinal Cord Injury Research Centre, Neuroscience Institute, Tehran University of Medical Sciences, Tehran, Iran (Islamic Republic of)

Synopsis

In this study, dynamic causal modeling (DCM) was applied to resting state fMRI data of mesial temporal lobe epilepsy (mTLE) patients to determine the directional alternations in effective connectivity in large scale brain networks. We hypothesized that mTLE alters the functional connectivity in both temporal and extra-temporal functional brain networks. We further hypothesized that the altered connectivity is directional (The direction between two network nodes matters). The results showed significantly different effective connectivity in default mode, limbic and salience networks.

Introduction

Mesial temporal lobe epilepsy (mTLE) is the most common type of focal epilepsy[1,2]. Psychological assessments and imaging approaches support the hypothesis that TLE is a network disorder[3,4]. We applied dynamic causal modeling (DCM) to resting state fMRI data of mTLE patients as well as healthy individuals to investigate how the large scale brain networks are altered by mTLE. We examined effective connectivity in four major brain networks, including default mode network (DMN) , attention network (ATN), salience network (SN) and limbic network (LIN).

Methods

Thirty-five unilateral patients were studied (21 left, 14 right mTLE; 19 females, 21 men; age range: 17-54; mean age 30.4 yrs). The resting-state fMRI data were preprocessed using the DPARSF 4.3 advanced edition based on SPM12: Images were realigned and corrected for head-motion artifacts The realigned functional volumes were spatially normalized to the MNI space using the normalization parameters estimated from T1 structural image (voxel size [3, 3, 3]). Then, the data were smoothed using Gaussian kernel (FWHM = 8 mm), detrended to remove linear trends, and temporally filtered (0.01– 0.08 Hz) to decrease the effect of low-frequency drifts. We used coordinates four resting-state networks[5]: default mode network (DMN), central executive network (CEN), attention network (ATN), salience network (SN) and limbic network (LIN). Fig. 1 lists the ROIs. The principal eigenvariates were computed from an 8-mm-radius sphere centered on the peak F-value for each region and adjusted for the confounds. The effective connectivity was calculated using standard Bayesian technique and generative dynamic causal models (DCM12)[6]. The average effective connectivity for each network were compared across the three groups using one-way ANOVA. P-value less than 0.05 were considered significant.

Results

One-way ANOVA conduced for normal, left TLE, right TLE showed no significant difference between the three groups in CEN. Fig.2 shows the regions of the model in each functional network along with effective connectivity values with significant connections between each pair of groups. Positive (negative) connectivity indicates that the source region stimulates (inhibits) the activity in the target region.

Conclusion

DCM shows that there is a significant alteration in network connectivity in mTLE patients compared to the control group; also between the left and right TLE groups. These results are in agreement with previous studies[7] that the connectivity values are directional in nature, regardless of temporal or extra temporal brain regions. Right lateral parietal in default mode network, amygdala in limbic network and left lateral parietal in salience network are the most significant nodes between the three groups. As a propagation point for many seizures, this may reflect downstream dysfunction in patients. These finding are consistent with important roles in seizure propagation, specifically for limbic regions for both temporal and extra temporal lobe epilepsy.

Acknowledgements

References

1. Engel J. Mesial Temporal Lobe Epilepsy: What Have We Learned? The Neuroscientist. 2001;7(4):340-352. doi:10.1177/107385840100700410

2. Téllez-Zenteno JF, Hernández-Ronquillo L. A Review of the Epidemiology of Temporal Lobe Epilepsy. Epilepsy Research and Treatment. 2012;2012:1-5. doi:10.1155/2012/630853

3. Chiang S, Stern JM, Engel J, Levin HS, Haneef Z. Differences in graph theory functional connectivity in left and right temporal lobe epilepsy. Epilepsy Research. 2014;108(10):1770-1781. doi:10.1016/j.eplepsyres.2014.09.023

4. Stretton J, Thompson PJ. Frontal lobe function in temporal lobe epilepsy. Epilepsy Research. 2012;98(1):1-13. doi:10.1016/j.eplepsyres.2011.10.009

5. Razi A, Seghier ML, Zhou Y, et al. Large-scale DCMs for resting-state fMRI. 2017;1. doi:10.1162/NETN

6. Friston K. Dynamic Causal Modelling (DCM) System System analyses analyses in in functional functional neuroimaging neuroimaging. (Dcm).

7. Bettus G, Guedj E, Joyeux F, et al. Decreased basal fMRI functional connectivity in epileptogenic networks and contralateral compensatory mechanisms. Human Brain Mapping. 2009;30(5):1580-1591. doi:10.1002/hbm.20625

Figures

	Default mode network	Abbreviation	Limbic	Abbreviation	Control executive network	Abbreviation	Salience network	Abbreviation
1	Posterior cingulate/ Precuneus	PcP	Left subgenual anterior cingulate cortex	LACC	Dorsal medial PFC	DmPFC	Dorsal anterior cingulate	DAC
2	Medial Prefrontal	MP	Right subgenual anterior cingulate cortex	RACC	Left anterior PFC	LaPFC	Left anterior PFC	LaPFC
3	Left lateral parietal	LLP	Left amygdala	LAMG	Right anterior PFC	RaPFC	Right anterior PFC	RaPFC
4	Right lateral parietal	RLP	Right amygdala	RAMG	Left superior parietal	LSP	Left insula	LI
5	Left inferior temporal	LIT	Left ventral hippocampus	LHIP	Right superior parietal	RSP	Right insula	RI
6	Right inferior temporal	RIT	Right ventral hippocampus	RHIP			Left lateral parietal	LLP
7	Medial dorsal thalamus	MDT					Right lateral parietal	RLP

Regions in Large-Scale Brain networks

Significant difference in effective connectivity between each pair of normal, left TLE, and right TLE groups in each network. Black lines indicate mean of the normal group, red lines indicated the mean of the left TLE groups and blue lines indicate the mean of the right TLE groups.

0955

Early detection of radiation-induced injury and prediction of cognitive deficit by MRS metabolites in radiotherapy of low grade glioma

Zahra Alirezaei[1,2], Mohammadreza Nazemzadeh[3], Masoud Hasanpour[3], Alireza Amouheidari[4], and Sajad Iraji[3]

[1]Isfahan University of Medical Sciences, Isfahan, Iran (Islamic Republic of), [2]Bushehr University of Medical Sciences, Bushehr, Iran (Islamic Republic of), [3]Tehran University of Medical Sciences, Tehran, Iran (Islamic Republic of), [4]Milad Hospital, Isfahan, Iran (Islamic Republic of)

Synopsis

To compare the sensitivity of alteration in MRS metabolites and MoCA and ACE-R cognitive tests in early and early-delayed post-radiation phases in detection of radiation-induced injury of Low Grade Glioam patients. The MRS metabolites, the ACE-R and MoCA, and the dosimetric parameters in the corpus callosum were analyzed during RT and up to 6-month post-RT for 10 LGG patients. NAA/Cr and Cho/Cr declined significantly at least 3 months before detecting alterations in ACE and MoCA cognitive tests. Therefore, the MRS-based biomarkers may be more sensitive than the state of the art cognitive test tools in prediction of post-radiation cognitive impairments.

Introduction

Radiation therapy (RT) plays a major role in treatment of low grade glioma (LGG) patients1. During RT, the brain normal tissue will inevitably be exposed to the radiation, causing radiation-induced brain injury (RIBI), classified as early, early-delayed, and late-delayed2,3. MR spectroscopy (MRS) can evaluate RIBI by assessing the metabolic concentrations of N-Acetylaspartate (NAA), Choline (Cho), and Creatine (Cr) 4,5. The corpus callosum (CC) is evidenced to be sensitive to the radiation effects leading cognitive decline6-8. Post-RT cognitive impairments are not commonly detectable by cognitive assessment tools such as the ACE, and MoCA in early-delayed phase9-11. This study aimed to investigate whether MRS metabolite variations can be a more sensitive tool for detecting RIBI in early post-radiation phase compared to conventional cognitive tools.

Methods

10 patients histologically confirmed with low grade glioma underwent craniotomy and RT without receiving chemotherapy. Standard 3D conformal radiotherapy was prescribed using 1.8 Gy in 30 fractions by ONCOR linear accelerators. All patients had MRI/MRS scans at the baseline, at the fourth week of RT, 1, 3 and 6-month after RT. The Farsi versions of the (MoCA-P) and (ACE-P) were completed by all patients at the time of their MRI scans. ACE-R includes attention/ orientation, memory, fluency, language, and visuospatial ability. MoCA-P contains visuospatial; naming; memory; language; abstraction; and attention domains. The significance of sequential deviations from the baseline values for the metabolic ratios of Cho/ Cr and NAA/Cr; and the ACE-R and MoCA results were inspected using a paired-sample Student's t test. All tests were two-tailed and conducted at the 5% significance level. The correlations between the metabolic ratios and ACE-R and MoCA scores were assessed by Pearson correlations. The correlation between the alterations in NAA/Cr and Cho/Cr in with the alterations in ACE-R and MoCA scores in consecutive time points was also inspected.

Results

Compared to the pre-RT values, NAA/Cr ratio decreased by 0.10±0.03 (P = 0.001), 0.12±0.05 (P = 0.04), 0.17±0.05 (P = 0.001) and 0.18±0.06 (P = 0.005) at the fourth week of RT, 1-month, 3-month and 6-month post- RT, respectively. Again compared to the pre-RT values, the mean of Cho/Cr ratio decreased by 0.12±0.05 (P = 0.0001), 0.15±0.03 (P = 0.0001), 0.24±0.06 (P = 0. 04), and 0.20±0.07 (P = 0.003) at the fourth week of RT, 1-month, 3-month and 6-month post-RT, respectively. Compared to the baseline values, both the MoCA and ACE-R scores taken 6-month post RT were statistically significant (P=0.0001 and 0.002). Overall, five and four patients had ACE-R and MoCA scores below the normal at 6-month post-RT, respectively. A significance decline was observed in MoCA language domain at 6-month compared to 3-month post-RT (P-value = 0.05). Also, there was a significant difference between MoCA language score at the 6-monnh follow up compared to the baseline value (P-Value=0.045). Furthermore, a significant decrease was seen between the score of MoCA memory subdomain at the 6-month post-RT to the baseline value (P-value= 0.04). ACE-R showed declines in language and verbal fluency subdomains for two patients at the 4th week of RT. However, both ACE-R and MoCA showed decline by both the language and verbal fluency subdomains at 6-month post-RT. Overall, ACE-R and MoCA tests showed cognitive declines for 6 patients, 6-month post-RT.

Discussion

Significant unremitting decline from fourth week of RT up to 6-month post-RT in NAA/Cr and Cho/Cr ratio confirmed the hypothesis that the microstructural metabolic changes in CC can predict cognitive declines at the early-delayed phase12. Significant changes in patient's MoCA and ACE-R scores at 3 and 6-month post-RT were observed, while abnormal score was reported for for patients with lower baseline scores, similar to the Brown et al. study13. A decline in language and verbal fluency, visuospatial and memory scores specifically at 3 and 6-month post-RT was demonstrated. The variation in the microstructure of the CC can strongly affect visuospatial perception and verbal fluency tasks, as well as other cognitive functions such as memory which may result in serious cognitive disorders 14-16. Mean delivered dose to the critical structures as one of the effective parameters on the white matter and consequently cognitive impairments showed a negative correlation with the deviation of NAA/Cr between pre-RT and 4th week of RT, and a negative correlation with the deviation of NAA/Cr between 4th week of RT and 1month post-RT. The dose dependence of the metabolic deviance in normal appearing brain tissue is a controversial issue confirmed by some studies, yet rejected by others17.

Conclusion

Significant variation of MRS metabolites in the corpus callosum started at early phases after RT of LGG patients up to early-delayed and delayed phases. Since the corpus callosum plays a critical role in most cognitive pathways, such early-delayed variation of metabolites can be considered a more sensitive predictor of long term detrimental effects of radiotherapy on cognitive functions, in comparison with ACE-R or MoCA. This study suggests that the MRS study of early variations in NAA/Cr and Cho/Cr in the corpus callosum may be exploited to modify the treatment plans for the patients and to design more sensitive cognitive assessment tools and introduce reliable quantitative imaging biomarkers that can predict cognitive decline in LGG patients before it manifests at the late-delayed stages.

Acknowledgements

No acknowledgement found.

References

1. Balentova S, Adamkov M. Molecular, cellular and functional effects of radiation-induced brain injury: a review. Int. J. Mol. Sci.. 2015;16(11):27796-815.

2. Robbins M, Greene-Schloesser D, Peiffer AM, Shaw E, Chan MD, Wheeler KT. Radiation-induced brain injury: A review. Front. Oncol.. 2012;2:73.

3. Béhin A, Delattre J-Y, editors. Complications of radiation therapy on the brain and spinal cord. Seminars in neurology; 2004.

4. Connor M, Karunamuni R, et al. Regional susceptibility to dose-dependent white matter damage after brain radiotherapy. Radiother Oncol. 2017;123(2):209-17.

5. Bobek-Billewicz B, Stasik-Pres G, Majchrzak H, Zarudzki L. Differentiation between brain tumor recurrence and radiation injury using perfusion, diffusion-weighted imaging and MR spectroscopy. Folia Neuropathol. 2010;48(2):81-92.

6. Di Paola M, Spalletta G, Caltagirone C. In vivo structural neuroanatomy of corpus callosum in Alzheimer's disease and mild cognitive impairment using different MRI techniques: a review. J Alzheimers Dis. 2010;20(1):67-95.

7. Thomann PA, Wüstenberg T, Pantel J, Essig M, Schröder J. Structural changes of the corpus callosum in mild cognitive impairment and Alzheimer's disease. Dement Geriatr Cogn Disord. 2006;21(4):215-20.

8. Yamauchi H, Fukuyama H, Shio H. Corpus callosum atrophy in patients with leukoaraiosis may indicate global cognitive impairment. Stroke. 2000;31(7):1515-20.

9. Fu X, Shrestha S, Sun M, Wu Q, Luo Y, Zhang X, et al. Microstructural White Matter Alterations in Mild Cognitive Impairment and Alzheimer's Disease. Clin. Neuroradiol. 2019.

10. Luo C, Li M, Qin R, Chen H, Yang D, Huang L, et al. White Matter Microstructural Damage as an Early Sign of Subjective Cognitive Decline. Front. Aging Neurosci. 2020;11(378).

11.Zhang M, Jin H, Sun S, Bu M, Su Q, Liu G, et al. Detection of radiation brain injury of malignant glioma by 1H-MRS. J. of Jilin University (Med Edition). 2011;37(4):742-5.

12. Greene-Schloesser D, Robbins ME, Peiffer AM, Shaw EG, Wheeler KT, Chan MD. Radiation-induced brain injury: A review. Frontiers in oncology. 2012;2:73-.

13. Brown PD, Buckner JC, et al. Effects of radiotherapy on cognitive function in patients with low-grade glioma measured by the folstein mini-mental state examination. J. Clin. Oncol.2003;21(13):2519-24.

14. Giorgio A, De Stefano N. Cognition in multiple sclerosis: relevance of lesions, brain atrophy and proton MR spectroscopy. Neurol. Sci. 2010;31(2):245-8.

15. Fryer SL, Frank LR, Spadoni AD, Theilmann RJ, Nagel BJ, Schweinsburg AD, et al. Microstructural integrity of the corpus callosum linked with neuropsychological performance in adolescents. Brain and cognition. 2008;67(2):225-33.

16. Kozlovskiy S, Vartanov A, Pyasik M, Nikonova E. Functional role of corpus callosum regions in human memory functioning.Int. J. Psychophysiol. 2012;3(85):396-7.

17. Sundgren P. MR spectroscopy in radiation injury. Am. J. Neuroradiol. 2009;30(8):1469-76.
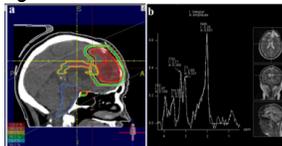
Figures

Figure 1. a: Isodose curves of a treatment plan of a LGG patient with a Left Frontal tumor on Prowess Panther 5.5; b: An example of MRS metabolite peaks of a voxel on the CC, fused with T2W MRI on a 1.5 Tesla Siemens Magnetom Aera scanner.
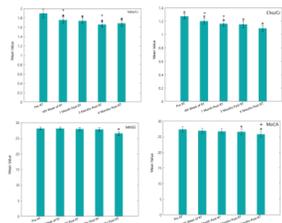

Figure 2. Plots of the mean percantage difference in the mean value of NAA/Cr and Cho/Cralong with the ACE and MoCA Scores at the 4th week of RT, 1-month, 3-month and 6-month post-RT, compared to the previous timepoints and baseline pre-RT values. The star markers show significant differences to the base line, while the plus ones present the significant differences between any parameters to its previous time point.